ACS OMEGA

http://pubs.acs.org/journal/acsodf

Article

Functionalization of Metal Surface via Thiol−Ene Click Chemistry: Synthesis, Adsorption Behavior, and Postfunctionalization of a Catechol- and Allyl-Containing Copolymer

Yucheng Zhang, Chien-Wei Chu, Wei Ma, and Atsushi Takahara*

Cite This: *ACS Omega* 2020, 5, 7488−7496

Read Online

ACCESS | Metrics & More | Article Recommendations | Supporting Information

ABSTRACT: Surface functionalization tailors the interfacial properties without impacts on the mechanical strength, which is beneficial for industry and daily applications of various metallic materials. Herein, a two-step surface functionalization strategy, (1) catechol-mediated immobilization of clickable agent and (2) postfunctionalization based on thiol−ene click reaction, is achieved using a copolymer, namely poly[2-(methacryloyloxy)ethylundec-10-enoate]-*co*-(*N*-(3,4-dihydroxyphenethyl) methacrylamide) [P(MEUE-*co*-DPMAm)]. To reduce the potential side reactions of allylic double bonds in allyl methacrylate during the polymerization, the MEUE are designed and synthesized with better control over the polymer chain growth. The surface functionalization via the two-step method is demonstrated using various thiols, e.g., hydrophobic, hydrophilic, and polymeric thiols under room conditions. Additionally, the hydrophobic-thiol-functionalized anodic aluminum oxide is found to be a candidate for the oil/water separation with a separation efficiency of ∼99.2%. This surface modifier provides practical insights into the further design of functional materials.

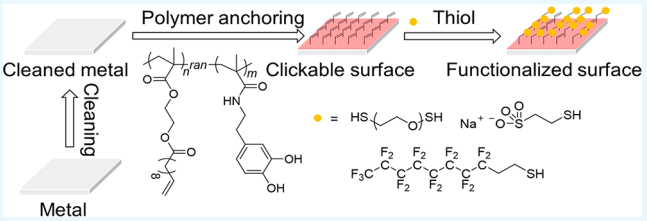

1. INTRODUCTION

Surface functionalization of metals and alloys, such as titanium, aluminum, nickel, and stainless steel (SUS), plays an important role in their applications ranging from daily to industrial uses.[1] As the physical and chemical properties (e.g., wettability, biocompatibility, antifouling, and anticorrosion properties) of polymers are tailorable through the structure design and synthesis strategies, polymeric surface modifiers are receiving increased attention.[2−4] For example, poly(dimethylsiloxane), a polymer with low surface free energy, has been coated on ship hulls to reduce the fouling of marine organisms and prevent corrosion in seawater.[3,4] However, the undesirable detachment of the polymer coatings from metal surfaces frequently occurs because the adhesion forces (originating from van der Waals interactions) are inherently weak. To address this issue, diverse synthetic polymers containing catechol units have been reported.[5,6] These types of surface modifiers with strong adhesion properties are biomimetic to the mussels. Mussels could anchor themselves to the rock or ship tightly, even under wet conditions. This astonishing adhesion effect is related to the existence of catechol groups in their adhesive proteins (e.g., Mfp-5).[7] Although the interactions between the catechol groups and the metals have not been thoroughly assessed so far, its good performance allows catechol-containing polymers to be highly promising surface modifiers.[5,6]

The preparation of polymers with catechol groups and desirable functionalities is a great challenge because of a complicated synthesis procedure, as well as their solubility and chemical stability during the synthesis and modification process.[8] Immobilizing a polymer with catechol groups and clickable agents and performing the postfunctionalization via click reactions could be a better approach. Click reactions refer to a set of covalent reactions, including azide−alkyne Huisgen 1,3-dipolar cycloaddition, Diels−Alder addition, and thiol−ene reaction, that have several attractive characteristics, such as easy occurrence, high efficiency, good specificity, and nearly quantitative yield.[9] Therefore, polymer modifiers containing clickable agents have been designed to introduce the desirable functionalities to the surface of materials.[10,11] Among various click reactions, thiol−ene click reaction is advantageous for surface functionalization: (1) the allyl is inert toward acid, base, ultraviolet (UV) light, and thermal energy;[12,13] (2) the reaction can be easily triggered by free radicals under ambient conditions without using expensive or toxic catalysts;[14−16] (3) if the radicals are generated by photoinitiation, many parameters, e.g., light intensity, exposure dose, and duration of the photoreactions, can be readily controlled.[14,17] Because of these outstanding characteristics, the thiol−ene click reaction was utilized to produce enzyme patterns on the glass surface.[17]

Received: January 19, 2020
Accepted: March 13, 2020
Published: March 26, 2020

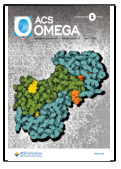

Herein, we reported a two-step surface functionalization strategy using a catechol- and allyl-containing copolymer, poly[2-(methacryloyloxy)ethylundec-10-enoate]-*co*-(*N*-(3,4-dihydroxyphenethyl) methacrylamide) [P(MEUE-*co*-DPMAm)]. The P(MEUE-*co*-DPMAm) was synthesized via a reversible addition−fragmentation chain-transfer (RAFT) polymerization; the introduction of 8-methylene spacer significantly reduced the side reactions of allylic double bonds during polymerization.[18−20] The clickable layer was formed onto metallic materials within 6 h of immersion in P(MEUE-*co*-DPMAm) solution. The thiol−ene click chemistry at the surface was demonstrated using hydrophobic, hydrophilic, and polymeric thiols. Furthermore, the anodic aluminum oxide (AAO) was utilized as an oil/water separation membrane after the two-step functionalization using a hydrophobic thiol. Our research may bring valuable insights into the design and functionalization of metal surfaces.

2. EXPERIMENTAL SECTION

2.1. Materials and Characterization. 3-Hydroxytyramine hydrochloride (98%), *tert*-butyldimethylchlorosilane (98%), methacryloyl chloride (90%, stabilized with 4-methoxyphenol), allyl methacrylate (AMA, 95%, stabilized with 4-methoxyphenol), and tetra-*n*-butylammonium fluoride solution (TBAF, 1 M tetrahydrofuran (THF) solution) were purchased from Tokyo Chemical Industry Co. (Japan) and used without any further purification. 2-Hydroxyethyl methacrylate (97%, stabilized with 4-methoxyphenol), dodec-11-enoyl chloride (97%), 4-cyano pentanoic acid dithiobenzoate (CPADB, 97%), 2,2′-azobis(2-methylpropionitrile) (AIBN, 98%), 1*H*,1*H*,2*H*,2*H*-perfluorodecane thiol (PFDT, 97%), 1-dodecanethiol (97%), sodium 2-mercaptoethanesulfonate (MESNa, 97%), poly(ethylene glycol) dithiol (PEG-SH, average M_n 3400), 2-hydroxy-1-[4-(hydroxyethoxy) phenyl]-2-methyl-1-propanone (Irgacure 2959, 97%), Oil Red O, and lithium bromide (LiBr, 99%) were obtained from Sigma-Aldrich Co. (Japan) and used directly. The solvents, including tetrahydrofuran (THF, HPLC grade, 99.9%), methanol (HPLC grade, 99.9%), hexane (HPLC grade, 99%), acetone (HPLC grade, 99%), dimethylformamide (DMF), dichloromethane (DCM), and chloroform (HPLC grade, 99%) were obtained from Wako Pure Chemicals Co. (Japan). Ultrapure water was prepared by a Millipore water purification system (Milli-Q system, Millipore, Japan). Four kinds of metal substrates (1 cm × 1 cm), specifically Al, Ti, Ni, and SUS, were provided by Nilaco Co. (Japan). AAO filters with diameters of 3 cm were purchased from Whatman (GE Health Care Co., Japan).

The structures of the monomers and the obtained polymers were elucidated by proton nuclear magnetic resonance (^{1}H NMR) spectroscopy (AVANCE III 400, Bruker Co., Germany). The number-average molecular weight (M_n) and polydispersity index (PDI) were measured by size exclusion chromatography (SEC system, JASCO Co., Japan) system at 0.5 mL/min at 40 °C using DMF with 0.05 M LiBr as the eluent. The monodisperse poly(methyl methacrylate) (PMMA) standards were utilized for the molecular-weight calibrations of resultant P(MEUE-*co*-DOPAm) and P(AMA-*co*-DOPAm) copolymers. The static contact angle data were obtained by a Theta T200 Auto3 contact angle instrument (Altech Co., Japan) at 25 °C in the open air using 2 μL of a water droplet as the probe, and all contact angle data was obtained by performing five independent measurements.[21] X-ray photoelectron spectroscopy (XPS) measurements were carried out on an APEX instrument (ULVAC-PHI, Inc., Japan) at 25 °C under 2×10^{-9} Torr with a take-off angle of 45°. An Al/Kα X-ray source at 150 W was utilized for the XPS measurement. A spectroscopic ellipsometer MASS-103FH (Five labs) was utilized to calculate the coating thicknesses before and after the click reaction. The data were collected using 50 fixed wavelengths ranging from 300 to 800 nm (10 nm increments) at a take-off angle of 70°. The thicknesses of the copolymer layers were calculated with an assumed refractive index of 1.52 at 632.8 nm.[22] The water content of the hexane after water/oil separation was evaluated using a Karl Fischer Moisture Titrator (MKC-710, Kyoto Electronics Manufacturing Co., Japan). The KEMAQUA Anolyte AGE and KEMAQUA Ctholyte CGE were utilized as anode and cathode solutions, respectively. Each sample was measured three times, and the average data are presented.

2.2. Synthesis of P(MEUE-*co*-DOPAm). *N*-(3,4-Bis((*tert*-butyldimethylsilyl)oxy)phenethyl) methacrylamide (DOPAm$_{TBDMS}$) was synthesized by the following steps. 3-Hydroxytyramine hydrochloride (9.5 g, 48 mmol) was dripped into *tert*-butyldimethylchlorosilane (17.3 g, 115 mmol) with imidazole (11.7 g, 173 mmol) in anhydrous DCM (40 mL). After a 6 h reaction at 25 °C, the mixture subsequently reacted with methacryloyl chloride (5.7 g, 55 mmol) at 25 °C for 6 h. 2-(Methacryloyloxy)ethyl undec-10-enoate (MEUE) was synthesized via acylation between 2-hydroxyethyl methacrylate (6.5 g, 50 mmol) and dodec-11-enoyl chloride (9.8 g, 45 mmol) using imidazole (3.4 g, 50 mmol) as an acid bonding agent in anhydrous DCM (25 mL) at 25 °C for 24 h.

A mixture of DOPAm$_{TBDMS}$ (1.12 g, 25.0 mmol), MEUE (2.13 g, 75.0 mmol), and CPADB (0.071 g, 0.25 mmol) in THF (3 mL) was bubbled with argon gas for 10 min. Subsequently, AIBN (8.2 mg, 0.05 mmol) was added into the solution to initiate the polymerization in a thermostatic oil bath at 60 °C for 24 h. After the resultant solution was poured into methanol and purified by reprecipitation, the P(MEUE-*co*-DOPAm$_{TBDMS}$) (82% yield) was obtained. The mixture of the resultant polymer (0.75 g) in THF (3 mL) and TBAF solution (0.1 mL) was then stirred for 6 h at 25 °C for deprotection. P(MEUE-*co*-DOPAm) (79% yield) was obtained by reprecipitation in methanol/water (3:1) and vacuum drying.

2.3. Formation of Clickable Layer. The clickable platforms were prepared by immersing substrates into the P(MEUE-*co*-DOPAm) solutions (5 mg/mL in THF). The metal plates (SUS, Al, Ti, and Ni) were sequentially cleaned by sonication in hexane, acetone, and ultrapure water for 10 min (two times for each solvent), followed by exposure of the substrates to vacuum ultraviolet (VUV) radiation for 20 min. The cleaned substrates were immersed in the P(MEUE-*co*-DOPAm) solutions under approximately neutral conditions for 6 h. The substrates and polymer solutions were then poured into THF (100 mL) and rinsed several times. After drying under vacuum, the modified substrates were characterized by the contact angle, spectroscopic ellipsometry, and XPS measurements.

2.4. Postfunctionalization via Click Chemistry. The postfunctionalization was performed using three types of thiols, e.g., hydrophobic, hydrophilic, and polymeric thiols. The hydrophobic thiol, PFDT (240 mg, 0.5 mmol), was dissolved with Irgacure 2959 (5.6 mg, 0.025 mmol) in 0.2 mL of chloroform, and the mixture was placed onto the P(MEUE-*co*-DOPAm)-immobilized substrates. A UV lamp (0.9 mW/cm^2 at 256 nm) irradiated the mixture and substrate for 20 min.

https://dx.doi.org/10.1021/acsomega.0c00259
ACS Omega 2020, 5, 7488−7496

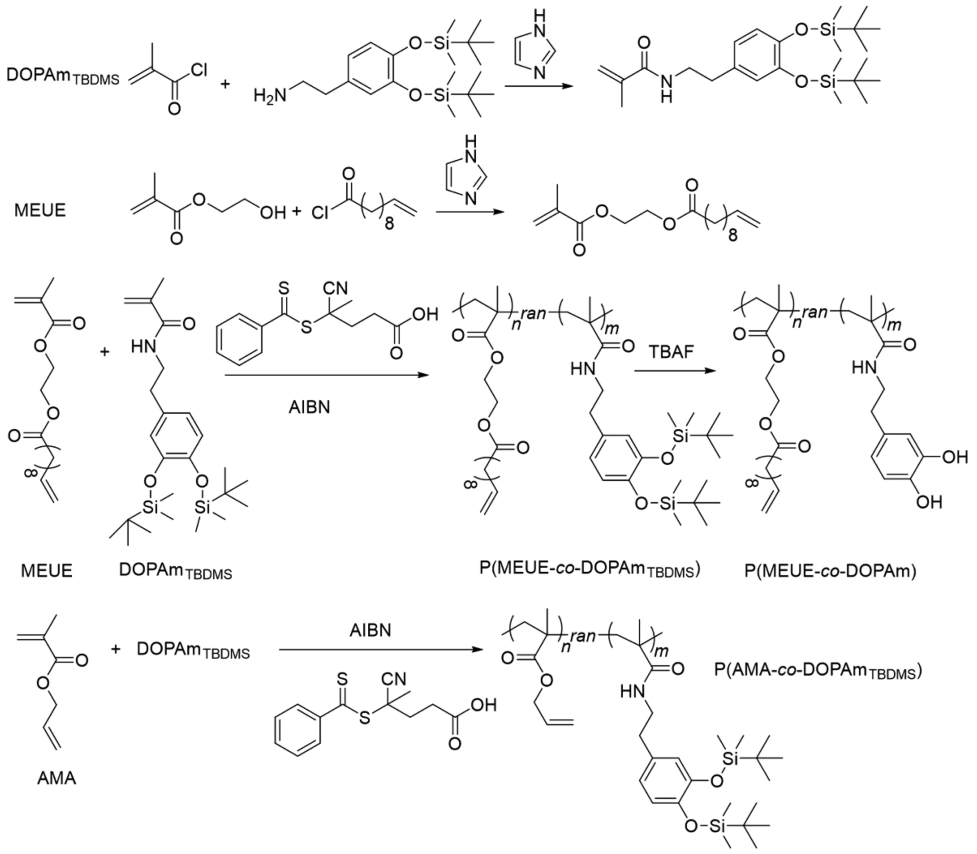

Figure 1. Synthetic strategy of P(MEUE-*co*-DOPAm), and P(AMA-*co*-DOPAm$_{TBDMS}$).

After the irradiation, the substrates were rinsed with chloroform to remove excess thiol reagents. Meanwhile, a control sample was designed using bare SUS substrates for the confirmation of the coating formation resulting from the adsorption of the PFDT molecule. A cleaned SUS plate after VUV treatment was immersed in PFDT solution (DMC) with Irgacure 2959, and the UV irradiation was applied for 20 min. The resultant samples were rinsed with DCM three times and dried under a vacuum state, namely, the control sample. The contact angle measurement was performed to confirm the adsorption of PFDT molecules. The hydrophilic thiol, MESNa (100 mg, 0.6 mmol), and Irgacure 2959 (7.2 mg, 0.03 mmol) were well-mixed in 1 mL of THF/water (v/v = 3:1) solution. The click reaction was performed under the same conditions as those used for PFDT functionalization. After irradiation, the substrates were rinsed with water to remove weakly adsorbed thiols. The surface click reaction of PEG-SH, a polymeric thiol, was performed in a THF/methanol (v/v = 2:1) polymer solution (300 mg of PEG-SH in 1 mL of the mixed solvent) with Irgacure 2959 (18.8 mg, 0.08 mmol) under UV irradiation as mentioned above. The polymer-grafted samples were carefully cleaned with water.

2.5. Oil/Water Separation Membrane. An AAO membrane was rinsed with hexane, acetone, and water, followed by VUV exposure for 20 min. The AAO membranes were immersed into the P(MEUE-*co*-DOPAm) solution (5 mg/mL in THF) solution for 6 h to prepare the clickable prelayer. The click reaction was further performed using PFDT (under the same conditions as described in Section 2.4) for 20 min. The surface wettabilities were evaluated by contact angle measurements. Surface-functionalized AAO membranes have been reported to serve as filters for the separations of various materials, such as metal cations, proteins, and organic compounds.[23] Here, the PFDT-modified hydrophobic AAO was utilized as a membrane for the hexane/water separation. The mixture of 5 mL water and 10 mL hexane was dyed in advance using an oil red O and poured to a Brinell funnel clamped with the PFDT-modified AAO filter, followed by filtration under reduced pressure. The solutions before and after the filtration were observed by an optical microscope. The separation efficiency was evaluated based on the Karl Fischer titration.[24] The purified hexane solution was mixed in anhydrous THF (weight ratio of W_{hexane}/W_{THF} is 5:4). After sonication, the water content of the mixture (C_m) was measured by the Karl Fischer moisture titrator. Moreover, the water content in anhydrous THF (C_{THF}) was measured by the titrator. The water content of hexane (C_H) was calculated using the following equation

$$C_H = (9 \times C_M - 4 \times C_{THF})/5 \quad (1)$$

Three purified hexane samples were measured by Karl Fischer titration, and the average water content was presented in this research.

3. RESULTS AND DISCUSSION

3.1. Synthesis of P(MEUE-*co*-DOPAm). The synthetic strategies of P(MEUE-*co*-DOPAm) are shown in Figure 1. The catechol-containing monomer (DOPAm$_{TBDMS}$) was introduced to PMEUE segments by RAFT polymerization. The catechol group is utilized in our work to enhance the interaction between the polymeric layer and metallic materials. This group possess an excellent adhesion effect for numerous

https://dx.doi.org/10.1021/acsomega.0c00259
ACS Omega 2020, 5, 7488−7496

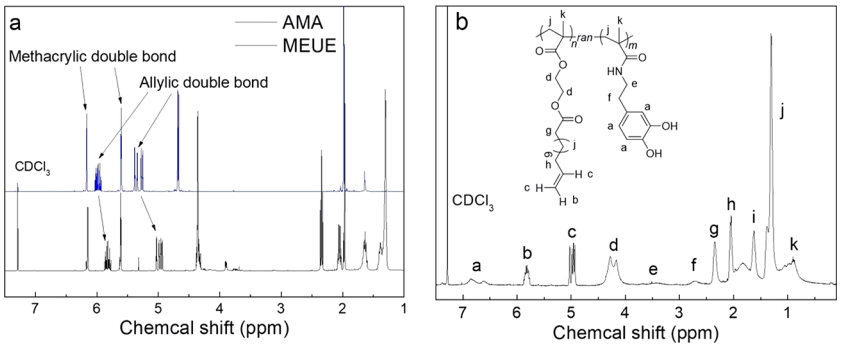

Figure 2. ^{1}H NMR spectra of (a) AMA and MEUE and (b) P(MEUE-*co*-DOPAm).

materials, including SUS, Al, Ti, and glass.[25−27] Notably, the catechol-containing polymers can dissolve in common organic solvents, which is advantageous for relativelylarge-scale production. However, the catechol group is unstable and self-polymerizable under alkaline conditions.[28−30] To address these issues, the free catechol groups are protected using TBDMS-Cl, and the monomer with the protected catechol groups, $DOPAm_{TBDMS}$, is synthesized. The chemical structures are evaluated by ^{1}H NMR measurements; all peaks in the spectrum (Figure S1) are readily assigned to their corresponding hydrogens and were consistent with previous findings.[25]

The thiol−ene click reaction is commonly performed using allylic, methacrylic, or methacrylamide double bonds.[28,31,32] Herein, the monomer with allylic double bonds is utilized because both methacrylic and methacrylamide double bonds are polymerizable during the introduction of catechol groups. Although the AMA with allylic double bonds is common and commercially available, both allylic and methacrylic double bonds in this monomer are reactive during the free radical polymerization, inducing the loss of clickable agent and uncontrollable polymerization;[18,19] in some reports, even the ratio of AMA is reduced to 20%, and the obtained copolymer still has a large PDI value.[19,20] Therefore, we attempt to reduce the reactions of the allylic double bond from the molecular design. As seen in Figure 1, there is only one methylene between allylic double bonds and ester groups, and the allylic double bonds are potentially influenced by the ester groups, inducing the reactivity during free radical polymerization. Hence, we designed a novel monomer with an 8-methylene spacer to isolate the allyl units from the ester group.

The difference of allylic double bonds in MEUE and AMA was revealed by ^{1}H NMR measurements. As shown in Figure 2a, the peaks of methacrylic double bonds show similar chemical shifts, while the chemical shifts of allylic double bonds in the MEUE (black curve) (∼5.81 and ∼4.97 ppm) are slightly shifted to a lower field than those in AMA monomer (blue curve) (∼5.97 and ∼5.34 ppm). These results suggest that the allylic double bonds in the MEUE are less influenced by ester groups than those in the AMA.

Both P(AMA-*co*-$DOPAm_{TBDMS}$) and P(MEUE-*co*-$DOPAm_{TBDMS}$) copolymers are prepared by RAFT polymerizations (Figure 1) under the same conditions (60 °C for 24 h), and the results are summarized in Table S1. The molecular weight and PDI of P(AMA-*co*-$DOPAm_{TBDMS}$) (26 300 g/mol and PDI ∼3.1) are much higher than the designed values (10 000 g/mol and PDI ∼1.0), whereas those of P(MEUE-*co*-$DOPAm_{TBDMS}$) (14 400 g/mol; PDI ∼1.5) are relatively closer to the designed values, demonstrating better control over polymer chain growth. Moreover, the content of catechol units in P(MEUE-*co*-$DOPAm_{TBDMS}$) is calculated at 27.0%, which is close to the feed ratio.

Moreover, we demonstrate that this reduction of activity during polymerization hardly influences the following thiol−ene click reaction. The thiol−ene click reaction was performed using PFDT as template thiol (see the Supporting Information for details), and a very high conversion (higher than 95%) of allyl units was obtained.

Eventually, P(MEUE-*co*-DOPAm) is obtained by the deprotection using TBAF in THF, and the formation of catechol groups increases the solubility of the resultant polymer in methanol; consequently, a mixture of methanol and water is utilized to precipitate the P(MEUE-*co*-DOPAm). The disappearance of the TBDMS signals in the ^{1}H NMR spectrum (0.23 and 1.02 ppm) (Figure 2b) indicates the achievement of complete deprotection.

3.2. Formation of Clickable Layer. The polymeric layer is prepared by immersing various substrates in the P(MEUE-*co*-DOPAm) solutions for 6 h. The immersion duration was optimized on the basis of the XPS and contact angle measurements (described in the Supporting Information).

After VUV treatment, all samples present a weak C_{1s} signal at 284 eV and a strong O_{1s} signal at 532 eV (Figure S6); these results imply that the surfaces are covered by the metallic oxide without organic contamination.[33] The atomic ratio between C_{1s} and O_{1s} (C/O) is calculated to give a semiquantitative evaluation (Table S4). The C/O ratios of SUS, Al, Ni, and Ti are 0.59, 0.24, 0.43, and 0.38, respectively. The immobilization of the P(MEUE-*co*-DOPAm) layer induces an increased intensity of the C_{1s} signal and a decreased intensity of the O_{1s} signal; the C/O ratios in all samples increase to 1.68 (SUS), 0.93 (Al), 1.81 (Ni), and 1.28 (Ti). These results indicate that the P(MEUE-*co*-DOPAm) layers are successfully formed onto the various metallic materials. As the theoretical C/O ratio of P(MEUE-*co*-DOPAm) is 4.2, the P(MEUE-*co*-DOPAm) layer is very thin and the O_{1s} signal from the metallic oxide contributed to the C/O ratio. Therefore, we performed spectroscopic ellipsometry using the SUS substrate as a template. The thickness of the polymer layer is ∼23 Å, indicating that the photoelectron from the metallic oxide can pass through the polymer layer and be observed in the XPS survey scan, thus affirming our suggestion.

More evidence can be provided by the high-resolution XPS profiles of C_{1s} and O_{1s}, as shown in Figures S7 and S8. All metals present similar high-resolution spectra regarding C_{1s} before the P(MEUE-*co*-DOPAm) adsorption. After cleaning, only one peak at ∼284.4 eV assigned to the C−C function is

https://dx.doi.org/10.1021/acsomega.0c00259
ACS Omega 2020, 5, 7488−7496

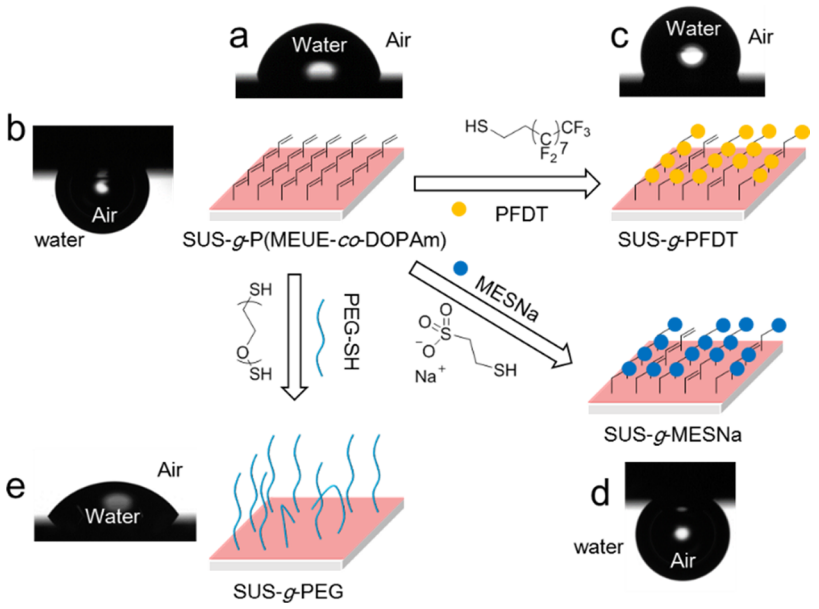

Figure 3. Scheme of the postfunctionalization of SUS-*g*-P(MEUE-*co*-DOPAm) using various thiols. The images of the water contact angle in the air for (a)SUS-*g*-P(MEUE-*co*-DOPAm), (c) SUS-*g*-PFDT, and (e) SUS-*g*-PEG and the air bubble contact angle in the water for (b) SUS-*g*-P(MEUE-*co*-DOPAm) and (d) SUS-*g*-MESNa were presented.

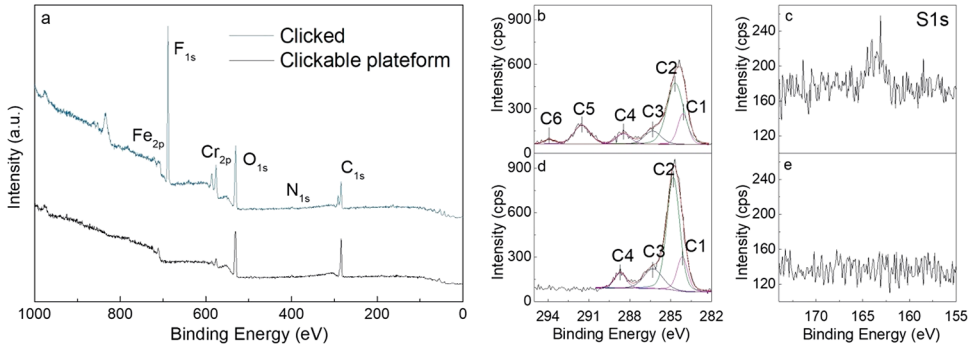

Figure 4. (a) XPS survey scan of the SUS-*g*-P(MEUE-*co*-DOPAm) before and after click reaction using PFDT as the template hydrophobic thiol. C_{1s} high-resolution scans of (b) clicked SUS and (d) clickable platform. S_{1s} high-resolution scans of (c) clicked SUS and (e) clickable platform.

seen in all metallic materials.[34] In the samples of P(MEUE-*co*-DOPAm)-grafted metals, the peak of C_{1s} split into four possible peaks (C1−C4) of the carbons atoms under different environments, where the peaks of C1 (284.4 eV), C2 (285.0 eV), C3 (287.0 eV), and C4 (289.4 eV) are assigned to the aromatic carbons, −C−C, −C−O, and −COO−, respectively.[35] The appearance of those peaks indicates that the P(MEUE-*co*-DOPAm) is adsorbed onto the metal surface. Conversely, the high-resolution spectra of O_{1s} for all cleaned metals are completely different, owing to the diverse binding energies of metallic oxides. Despite the initial signals from metallic oxides, two extra peaks at 531.8 and 533.2 eV are assigned to C−O and C═O, respectively.[36] Because the organic oxygen exists only in the copolymer, the polymer modification is achieved successfully.

The polymer adsorption also induces significant changes in the surface wettability, and the contact angles are shown in Table S5. Before the modification, the metal surface is superhydrophilic. The cleaned metal surface with high surface free energy is easily wetted by water. After the polymer immobilization, the contact angles increase to ∼83.7, ∼83.0, ∼77.9, and ∼81.7° in SUS, Al, Ni, and Ti samples, respectively. Since the metal surface is segregated by the hydrophobic P(MEUE-*co*-DOPAm) layers, the wettability of water droplets reduces and a high contact angle is observed. Moreover, the polymer uniformly adsorbs to the metallic materials (Figure S5). Since the thickness of resultant film prepared by "grafting-to" method is influenced by the immersion duration and molecular weight of the synthesized copolymer, this modification strategy has good control over the film thickness and morphology.[37]

3.3. Postfunctionalization via Click Chemistry. After modification, the surface of the clickable platform is segregated by the allylic double bonds, which enable the thiol−ene click reaction. As shown in Figure 3, SUS-*g*-P(MEUE-*co*-DOPAm) is utilized as a template to prove the surface click reaction using hydrophobic, hydrophilic, and polymeric thiols. PFDT is a kind of thiol that contains perfluorooctyl with strong hydrophobicity. Although perfluoroalkanes are harmful to the environment and the human body, we use this molecule to illustrate the advantages of postfunctionalization because of the complex synthesis and poor solubility of perfluorooctyl-containing surface modifiers.[38] The hydrophilic modification is achieved using MESNa as a functionality. This molecule,

https://dx.doi.org/10.1021/acsomega.0c00259
ACS Omega 2020, 5, 7488−7496

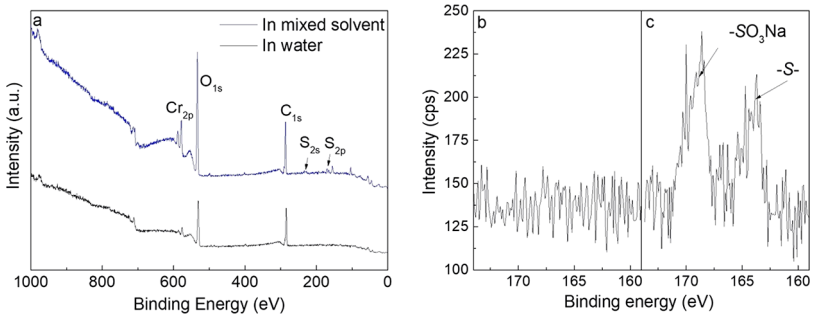

Figure 5. (a) XPS survey scan of SUS-*g*-P(MEUE-*co*-DOPAm) after click reaction in water and water/THF mixture using MESNa as a template hydrophilic thiol. S_{2p} high-resolution scans of clicked SUS using (b) water and (c) mixed solution as solvents.

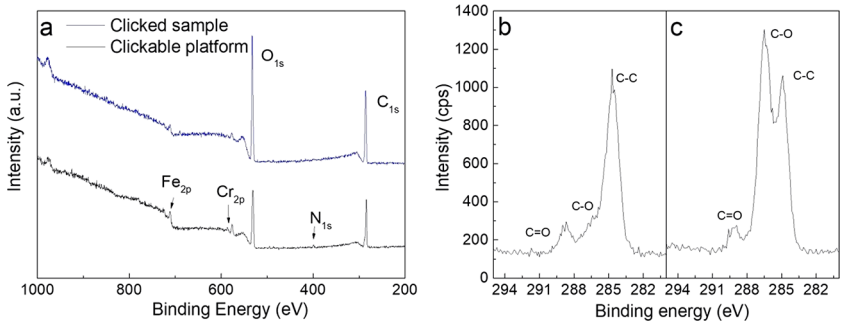

Figure 6. (a) XPS survey scan of SUS-*g*-P(MEUE-*co*-DOPAm) before and after click reaction using PEG-SH as the template polymeric thiol. C_{1s} high-resolution scans of SUS-*g*-P(MEUE-*co*-DOPAm) (b) before and (c) after the click reaction.

containing both an anion and a cation, possesses strong hydrophilicity and cation detectability.[39,40] Besides the functionalization using the small molecules with thiol groups, the polymer grafting via thiol−ene click reaction is also achieved using a type of polymeric thiol (PEG-SH). The PEG-SH consists of poly(ethylene glycol) (PEG) in its main chain, and PEG is a kind of functionality in reducing nonspecific biomolecule adsorption.[41,42]

The postfunctionalization of SUS-*g*-P(MEUE-*co*-DOPAm) using PFDT is achieved using Irgacure 2959 as the photoinitiator in chloroform under 20 min UV exposure (Figure S2). The duration period of UV exposure is optimized on the basis of contact angle measurement. The XPS survey spectra of the surface before and after PFDT functionalization are presented in Figure 4a.

After the click reaction, a new peak of F_{1s} at 688 eV appears, both the intensity and shapes of the C_{1s} change, and the C/O ratio slightly increases from 1.68 to 1.81.[35] Two additional peaks corresponding to $-CF_2-$ (C5, 291.7 eV) and $-CF_3$ (C6, 294.1 eV) appear in the C_{1s} high-resolution spectra of SUS-*g*-PFDT (Figure 4b).[43] In the high-resolution spectra of S_{2p}, no peak is identified from the SUS-*g*-P(MEUE-*co*-DOPAm) samples (Figure 4e); after the click reaction, there is a weak peak at 162 eV, which is assigned to the −S− functions (Figure 4c).

Moreover, the thicknesses of the polymer layers are measured to be ∼35 Å by spectroscopic ellipsometry after PFDT modification. As the thickness of the P(MEUE-*co*-DOPAm) layer is ∼23 Å, the PFDT layer is ∼12 Å, which is in accordance with previous findings.[44] Meanwhile, the contact angle increases from 83.7° (SUS-*g*-P(MEUE-*co*-DOPAm)) to 112.4° (SUS-*g*-PFDT). These results reveal that the surface functionalization using PFDT could be achieved by the photoinitiated thiol−ene click reaction.

Meanwhile, a control sample was prepared using bare SUS substrates. After UV irradiation, a low contact angle (52.0 ± 3.1°) is observed. Although the cleaned SUS with high surface free energy promotes the adsorption of PFDT molecules, the poor thiol/metal interaction induces desorption during the rinsing procedure. Because of this, the formation of polymeric layer resulting from the direct adsorption of PFDT is negligible.

The surface functionalization of MESNa is characterized by XPS measurements (Figure 5). As MESNa is difficult to be dissolved into organic solvents, we tried to perform this reaction using pure water as the solvent. Although Irgacure 2959 shows acceptable solubility in water, the sulfur element is difficult to be distinguished in its survey scan (Figure 5a, black line) and the high-resolution scan of S_{2p} (Figure 5b), showing the failure of modification. The poor solubility of the hydrophobic allylic double bonds in water might inhibit the thiol−ene click reaction. Therefore, we introduced THF, a good solvent of MEUE segments, into the MESNa water solution. No precipitation is observed until the volume fraction of the added THF is three times higher than that of water. This mixture aids us in obtaining the MESNa-functionalized SUS surface. As shown in Figure 5a, two new peaks of sulfur are observed, which correspond to S_{2s} (233.2 eV) and S_{2p} (169.1 eV); the high-resolution spectrum of S_{2p} displays two peaks at 165.1 and 169.9 eV, which is similar to previous findings of the sulfur elements in a MESNa self-assembled monolayer.[45]

Although the thicknesses of the MESNa layers were evaluated by spectroscopic ellipsometry, we failed to obtain a precise value from the fitting. The short-chained MESNa molecules have a low impact on the thickness of the polymer layer, and the increased value is smaller than the error. Meanwhile, the air bubble contact angle inside the water is performed to elucidate the modification of MESNa. Before the

https://dx.doi.org/10.1021/acsomega.0c00259
ACS Omega 2020, 5, 7488−7496

modification, the surface with strong hydrophobicity possesses a relatively low air contact angle in the water at ∼109.8° (Figure 3a). The introduction of MESNa causes the contact angle to increase to ∼148.1° (Figure 3d) because the hydrophilic surface is difficult to be wetted by the air bubble inside water.[2]

As mentioned above, the solvent is required to dissolve both MEUE and thiol; the modification using PEG-SH is performed using a solution of THF/methanol (v/v = 2:1). The results of the polymer grafting are evaluated using XPS measurements, and the spectra are shown in Figure 6. In the spectra of the survey scan (Figure 6a), the peaks of Fe_{2p} and Cr_{2p} in SUS-*g*-P(MEUE-*co*-DOPAm) (black curve) disappear in SUS-*g*-PEG (blue curve). Moreover, we found that the C/O ratios increase from 1.68 to 1.81, which is slightly lower than the theoretical value of the PEG segment (2.0). In the high-resolution scan of C_{1s}, the intensity of the peak at ∼286.6 eV corresponding to the C−O function significantly strengthens in the SUS-*g*-PEG samples (Figure 6b).

The spectroscopic ellipsometry indicates that the thickness of the PEG layer was ∼30 Å. These reactively thick PEG brushes attenuate the photoelectrons from the metal surface. Moreover, if we assume that the density of the PEG segments was ∼1.09 g/cm^3, the grafting density of the PEG brushes could be estimated to be ∼0.51 chains/nm^2 based on Avogadro constant. This value is only slightly lower than the value of another attempt to introduce the PEG brushes onto silicon substrates by grafting-to method.[42] The water contact angle measurement in the air was performed to evaluate the surface wettability. The value decreased from ∼83.7° (SUS-*g*-P(MEUE-*co*-DOPAm)) (Figures 3a) to 49.8° (SUS-*g*-PEG) (Figure 3e). These results indicate the presence of the PEG brushes on the P(MEUE-*co*-DOPAm) surface. Because the thiol-terminated polymers can easily prepare by RAFT polymerization and the subsequent aminolysis of the dithioester groups, this two-step synthesis strategy of polymeric thiol allows the grafting of desirable polymer brushes.[46]

Moreover, this method is demonstrated to be versatile: the functionalization of four types of common metallic materials is achieved, e.g., SUS, Al, Ni, and Ti. The detailed reaction conditions and results of the functionalization of various metals using PFDT as the template thiol can be found in the Supporting Information.

3.4. Oil/Water Separation Membrane. An AAO membrane contains parallel through-hole cylindrical nanopores, and the surface functionalization has a great impact on its applications.[47,48] Herein, we modify the AAO membrane by PFDT using the two-step modification method under the above-mentioned conditions. The surface wettability is characterized by water contact angle measurements. The contact angle data for the VUV-treated AAO membrane are hard to obtain because of the immediate introduction of water into the AAO pores; hence, the contact angle value for the pretreated samples is not presented. The contact angles of AAO-*g*-P(MEUE-*co*-DOPAm) (∼114.2°) and AAO-*g*-PFDT (∼140.0°) are shown in Figure 7a,b, respectively. The values are far greater than those on the flat metal substrate, for example, 83° for the Al-*g*-P(MEUE-*co*-DOPAm) and 113° for the Al-*g*-PFDT. The theoretical contact angles of AAO-*g*-P(MEUE-*co*-DOPAm) and AAO-*g*-PFDT are calculated at 116.3 and 136.5°, respectively, using the Cassie−Baxter equation (the calculation method described in the Supporting Information). Similar values between the measured data and the calculated data illustrate the successful functionalization on the AAO membranes.

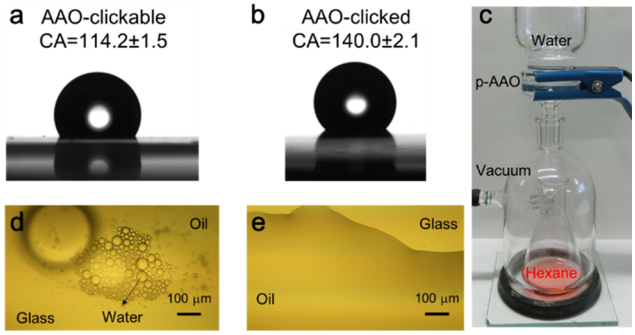

Figure 7. Contact angles of (a) P(MEUE-*co*-DOPAm)-modified AAO and (b) PDFT-modified AAO membranes using 2 μL water droplets as the probes. (c) Pictures of the instruments used for the water/oil separation test. The microscopy observations of the water/oil mixed solution (d) before and (e) after the separation.

Meshes or porous films with high water-in-air or oil-in-water contact angles could serve as filters for oil/water separation.[49] Here, the PFDT-clicked AAO membrane acts as a filter for hexane/water separation using a simple filtration setup, as shown in Figure 7c. The volume of the filtrated red solution is similar to the initial volume of hexane. The performance separation is evaluated using an optical microscope. Numerous water droplets in the hexane phase can be observed in Figure 7d, regarding the solution before the filtration, while only one hexane phase appears after purification (Figure 7e). Moreover, the water content is calculated from the Karl Fischer titration and the results indicate that the hexane contains ∼0.25 wt % water after separation. Considering that the water content is ∼33 wt % before the separation, the separation efficiency is ∼99.2%.

4. CONCLUSIONS

The P(MEUE-*co*-DOPAm) containing catechol and allyl groups is successfully synthesized and used as a surface modifier on various metallic materials to achieve postfunctionalization. The clickable prelayers are formed on the surfaces of various metallic materials, e.g., SUS, Al, Ni, Ti, and AAO, within a 6 h of immersion of materials in the polymer solutions, resulting from catechol-anchoring. The effective postfunctionalization is demonstrated via the photoinitiated thiol−ene click reactions using hydrophobic (PFDT), hydrophilic (MESNa), and polymeric (PEG-SH) thiols. The performance of this two-step method is similar for various metallic materials. Moreover, a successful separation of the hexane/water mixture using PFDT-clicked AAO membranes indicates that this surface modifier might provide practical insights into the further design of the functionalization for metallic materials.

■ ASSOCIATED CONTENT

Supporting Information

The Supporting Information is available free of charge at https://pubs.acs.org/doi/10.1021/acsomega.0c00259.

Synthesis and characterization of P(MEUE-*co*-DOPAm$_{TBDMS}$) and P(AMA-*co*-DOPAm$_{TBDMS}$); thiol−ene click reaction of P(MEUE-*co*-DOPAm$_{TBDMS}$) under solution state; adsorption behavior of P(MEUE-*co*-

https://dx.doi.org/10.1021/acsomega.0c00259
ACS Omega 2020, 5, 7488−7496

DOPAm); surface thiol−ene click reaction using hydrophobic thiol on four types of metallic materials; contact angle analysis of MESNa-clicked SUS sample; and calculation of the contact angle on AAO surface (PDF)

AUTHOR INFORMATION

Corresponding Author

Atsushi Takahara − *Institute for Materials Chemistry and Engineering and International Institute for Carbon-Neutral Energy Research (WPI-I 2CNER), Kyushu University, Fukuoka 819-0395, Japan*; orcid.org/0000-0002-0584-1525; Email: takahara@cstf.kyushu-u.ac.jp

Authors

Yucheng Zhang − *Institute for Materials Chemistry and Engineering, Kyushu University, Fukuoka 819-0395, Japan*

Chien-Wei Chu − *Institute for Materials Chemistry and Engineering, Kyushu University, Fukuoka 819-0395, Japan*

Wei Ma − *Institute for Materials Chemistry and Engineering and International Institute for Carbon-Neutral Energy Research (WPI-I 2CNER), Kyushu University, Fukuoka 819-0395, Japan*

Complete contact information is available at: https://pubs.acs.org/10.1021/acsomega.0c00259

Notes

The authors declare no competing financial interest.

ACKNOWLEDGMENTS

This research was partly supported by the JSTMirai Program (JPMJMI18A2).

REFERENCES

(1) Kango, S.; Kalia, S.; Celli, A.; Njuguna, J.; Habibi, Y.; Kumar, R. Surface Modification of Inorganic Nanoparticles for Development of Organic-Inorganic Nanocomposites-A Review. *Prog. Polym. Sci.* **2013**, *38*, 1232−1261.

(2) Kobayashi, M.; Terayama, Y.; Kikuchi, M.; Takahara, A. Chain Dimensions and Surface Characterization of Superhydrophilic Polymer Brushes with Zwitterion Side Groups. *Soft Matter* **2013**, *9*, 5138−5148.

(3) Nendza, M. Hazard Assessment of Silicone Oils (Polydimethylsiloxanes, PDMS) Used in Antifouling-/Foul-Release-Products in the Marine Environment. *Mar. Pollut. Bull.* **2007**, *54*, 1190−1196.

(4) Sommer, S.; Ekin, A.; Webster, D. C.; Stafslien, S. J.; Daniels, J.; VanderWal, L. J.; Thompson, S. E.; Callow, M. E.; Callow, J. A. A Preliminary Study on the Properties and Fouling-Release Performance of Siloxane-Polyurethane Coatings Prepared from Poly(dimethylsiloxane) (PDMS) Macromers. *Biofouling* **2010**, *26*, 961−972.

(5) Xu, H.; Nishida, J.; Ma, W.; Wu, H.; Kobayashi, M.; Otsuka, H.; Takahara, A. Competition between Oxidation and Coordination in Cross-Linking of Polystyrene Copolymer Containing Catechol Groups. *ACS Macro Lett.* **2012**, *1*, 457−460.

(6) Lee, H.; Dellatore, S. M.; Miller, W. M.; Messersmith, P. B. Mussel-Inspired Surface Chemistry for Multifunctional Coatings. *Science* **2007**, *318*, 426−430.

(7) Papov, V. V.; Diamond, T. V.; Biemann, K.; Waite, J. H. Hydroxyarginine-Containing Polyphenolic Proteins in the Adhesive Plaques of the Marine Mussel *Mytilus edulis*. *J. Biol. Chem.* **1995**, *270*, 20183−20192.

(8) Zhang, Y.; Hirai, T.; Ma, W.; Higaki, Y.; Kojio, K.; Takahara, A. Synthesis of a Bioinspired Catechol/Phosphorylcholine Surface Modifier and Characterization of its Surface Properties. *J. Polym. Sci., Part A: Polym. Chem.* **2018**, *56*, 38−49.

(9) Hoyle, C. E.; Lowe, A. B.; Bowman, C. N. Thiol-Click Chemistry: a Multifaceted Toolbox for Small Molecule and Polymer Synthesis. *Chem. Soc. Rev.* **2010**, *39*, 1355−1387.

(10) Madaan, N.; Terry, A.; Harb, J.; Davis, R. C.; Schlaad, H.; Linford, M. R. Thiol-Ene-Thiol Photofunctionalization of Thiolated Monolayers with Polybutadiene and Functional Thiols, Including Thiolated DNA. *J. Phys. Chem. C* **2011**, *115*, 22931−22938.

(11) Hensarling, R. M.; Doughty, V. A.; Chan, J. W.; Patton, D. L. "Clicking" Polymer Brushes with Thiol-yne Chemistry: Indoors and Out. *J. Am. Chem. Soc.* **2009**, *131*, 14673−14675.

(12) Fan, W.; Leclerc, M. K.; Waymouth, R. M. Alternating Stereospecific Copolymerization of Ethylene and Propylene with Metallocene Catalysts. *J. Am. Chem. Soc.* **2001**, *123*, 9555−9563.

(13) Choo, T. N.; Waymouth, R. M. The Dual-Site Alternating Cyclocopolymerization of 1,3-Butadiene with Ethylene. *J. Am. Chem. Soc.* **2003**, *125*, 8970−8971.

(14) Hoyle, C. E.; Bowman, C. N. Thiol−Ene Click Chemistry. *Angew. Chem., Int. Ed.* **2010**, *49*, 1540−1573.

(15) Khire, V. S.; Yi, Y.; Clark, N. A.; Bowman, C. N. Formation and Surface Modification of Nanopatterned Thiol-ene Substrates using Step and Flash Imprint Lithography. *Adv. Mater.* **2008**, *20*, 3308−3313.

(16) Campos, L. M.; Killops, K. L.; Sakai, R.; Paulusse, J. M. J.; Damiron, D.; Drockenmuller, E.; Messmore, B. W.; Hawker, C. J. Development of Thermal and Photochemical Strategies for Thiol-Ene Click Polymer Functionalization. *Macromolecules* **2008**, *41*, 7063−7070.

(17) Buhl, M.; Vonhoren, B.; Bavoo, B. J. Immobilization of Enzymes via Microcontact Printing and Thiol-Ene Click Chemistry. *Bioconjugate Chem.* **2015**, *26*, 1017−1020.

(18) Mennicken, M.; Nagelsdiek, R.; Keul, H.; Hocker, H. ATRP of Allyl Methacrylate with Alkyl Methacrylates-Crosslinking of Poly(methacrylate)s with Allyl Ester Side Groups. *Macromol. Chem. Phys.* **2004**, *205*, 2429−2437.

(19) Matsumoto, A.; Asai, S.; Aota, H. Free-Radical Crosslinking Polymerization of Unsymmetrical Divinyl Compounds, 1 Gelation in the Polymerization of Allyl Methacrylate. *Macromol. Chem. Phys.* **2000**, *201*, 2735−2741.

(20) Nagelsdiek, R.; Mennicken, M.; Maier, B.; Keul, H.; Holcker, H. Synthesis of Polymers Containing Cross-Linkable Groups by Atom Transfer Radical Polymerization: Poly(allyl methacrylate) and Copolymers of Allyl Methacrylate and Styrene. *Macromolecules* **2004**, *37*, 8923−8932.

(21) Honda, K.; Morita, M.; Sakata, O.; Sasaki, S.; Takahara, A. Effect of Surface Molecular Aggregation State and Surface Molecular Motion on Wetting Behavior of Water on Poly(fluoroalkyl methacrylate) Thin Films. *Macromolecules* **2010**, *43*, 454−460.

(22) Sugimoto, K.; Matsuda, S.; Ogiwara, Y.; Kitamura, K. Microscopic Ellipsometric Observation of the Change in Passive Film on 18Cr-8Ni Stainless Steel with the Initiation and Growth of Pit. *J. Electrochem. Soc.* **1985**, *132*, 1791−1795.

(23) Lee, W.; Park, S. Porous Anodic Aluminum Oxide: Anodization and Templated Synthesis of Functional Nanostructures. *Chem. Rev.* **2014**, *114*, 7487−7556.

(24) Cai, Y.; Chen, D.; Li, N.; Xu, Q.; Li, H.; He, J.; Lu, J. A Facile Method to Fabricate a Double-Layer Stainless Steel Mesh for Effective Separation of Water-in-Oil Emulsions with High Flux. *J. Mater. Chem. A* **2016**, *4*, 18815−18821.

(25) Gulley-Stahl, H.; Hogan, P. A.; Schmidt, W. L.; Wall, S. J.; Buhrlage, B.; Bullen, H. A. Surface Complexation of Catechol to Metal Oxides: An ATR-FTIR, Adsorption, and Dissolution Study. *Environ. Sci. Technol.* **2010**, *44*, 4116−4121.

(26) Mian, S. A.; Saha, L. C.; Jang, J.; Wang, L.; Gao, X.; Nagase, S. Density Functional Theory Study of Catechol Adhesion on Silica Surfaces. *J. Phys. Chem. C* **2010**, *114*, 20793−20800.

(27) Xu, Z. Mechanics of Metal-catecholate Complexes: The Roles of Coordination State and Metal Types. *Sci. Rep.* **2013**, *3*, No. 2914.

(28) Wang, L.; Li, G.; Lin, Y.; Zhang, Z.; Chen, Z.; Wu, S. A Strategy for Constructing Anti-adhesion Surfaces based on Interfacial Thiol−ene Photoclick Chemistry between DOPA Derivatives with a Catechol Anchor Group and Zwitterionic Betaine Macromolecules. *Polym. Chem.* **2016**, *7*, 4964−4974.
(29) Ball, V.; Frari, D. D.; Toniazzo, V.; Ruch, D. Kinetics of Polydopamine Film Deposition as a Function of pH and Dopamine Concentration: Insights in the Polydopamine Deposition Mechanism. *J. Colloid Interface Sci.* **2012**, *386*, 366−372.
(30) Glass, P.; Chung, H.; Washburn, N. R.; Sitti, M. Enhanced Reversible Adhesion of Dopamine Methacrylamide-Coated Elastomer Microfibrillar Structures under Wet Conditions. *Langmuir* **2009**, *25*, 6607−6612.
(31) Cai, T.; Wang, R.; Neoh, K. G.; Kang, E. T. Functional Poly(vinylidene fluoride) Copolymer Membranes via Surface-initiated Thiol−ene Click Reactions. *Polym. Chem.* **2011**, *2*, 1849−1858.
(32) Tucker-Schwartz, A. K.; Richard, A. F.; Robin, L. G. Thiol-ene Click Reaction as a General Route to Functional Trialkoxysilanes for Surface Coating Applications. *J. Am. Chem. Soc.* **2011**, *133*, 11026−11029.
(33) McCafferty, E.; Wightman, J. P. Determination of the Concentration of Surface Hydroxyl Groups on Metal Oxide Films by a Quantitative XPS Method. *Surf. Interface Anal.* **1998**, *26*, 549−564.
(34) Giesbers, M.; Marcelis, A. T. M.; Zuilhof, H. Simulation of XPS C1s Spectra of Organic Monolayers by Quantum Chemical Methods. *Langmuir* **2013**, *29*, 4782−4788.
(35) Cecchet, F.; Pilling, M.; Hevesi, L.; Schergna, S.; Wong, J. K. Y. G.; Clarkson, J.; Leigh, D. A.; Rudolf, P. Grafting of Benzylic Amide Macrocycles onto Acid-Terminated Self-Assembled Monolayers Studied by XPS, RAIRS, and Contact Angle Measurements. *J. Phys. Chem. B* **2003**, *107*, 10863−10872.
(36) Im, J.; Chandekar, A.; Whitten, J. E. Anomalous Vapor Sensor Response of a Fluorinated Alkylthiol-Protected Gold Nanoparticle Film. *Langmuir* **2009**, *25*, 4288−4292.
(37) Emilsson, G.; Schoch, R. L.; Feuz, L.; Höök, F.; Lim, R. Y. H.; Dahlin, A. B. Strongly Stretched Protein Resistant Poly(ethylene glycol) Brushes Prepared by Grafting-to. *ACS Appl. Mater. Interfaces* **2015**, *7*, 7505−7515.
(38) Tuminello, W. H.; Dee, G. T.; McHugh, M. A. Dissolving Perfluoropolymers in Supercritical Carbon Dioxide. *Macromolecules* **1995**, *28*, 1506−1510.
(39) Kudelski, A.; Pecul, M.; Bukowska, J. Interaction of 2-Mercaptoethanesulfonate Monolayers on Silver with Sodium Cations. *J. Raman Spectrosc.* **2002**, *33*, 796−800.
(40) Piotrowski, P.; Bukowska, J. 2-Mercaptoethanesulfonate (MES) Anion-Functionalized Silver Nanoparticles as an Efficient SERS-Based Sensor of Metal Cations. *Sens. Actuators, B* **2015**, *221*, 700−707.
(41) Cha, T. W.; Boiadjiev, V.; Lozano, J.; Yang, H.; Zhua, X. Immobilization of Oligonucleotides on Poly(ethylene glycol) Brush-Coated Si Surfaces. *Anal. Biochem.* **2002**, *311*, 27−32.
(42) Zdyrko, B.; Klep, V.; Luzinov, I. Synthesis and Surface Morphology of High-Density Poly(ethylene glycol) Grafted Layers. *Langmuir* **2003**, *19*, 10179−10187.
(43) Yuan, S. J.; Pehkonen, S. O. Microbiologically Influenced Corrosion of 304 Stainless Steel by Aerobic Pseudomonas NCIMB 2021 Bacteria: AFM and XPS study. *Colloids Surf., B* **2007**, *59*, 87−99.
(44) Patois, T.; Taouil, A. E.; Lallemand, F.; Carpentier, L.; Roizard, X.; Hihn, J.; Bondeau-Patissier, V.; Mekhalif, Z. Microtribological and Corrosion Behaviors of 1H,1H,2H,2H-Perfluorodecanethiol Self-Assembled Films on Copper Surfaces. *Surf. Coat. Technol.* **2010**, *205*, 2511−2517.
(45) Porter, M. D.; Bright, T. B.; Allara, D. L.; Chidsey, C. E. D. Spontaneously Organized Molecular Assemblies. 4. Structural Characterization of n-Alkyl Thiol Monolayers on Gold by Optical Ellipsometry, Infrared Spectroscopy, and Electrochemistry. *J. Am. Chem. Soc.* **1987**, *109*, 3559−3568.
(46) Carlini, L.; Fasolato, C.; Postorino, P.; Fratoddi, I.; Venditti, I.; Testa, G.; Battocchio, C. Comparison between Silver and Gold Nanoparticles Stabilized with Negatively Charged Hydrophilic Thiols: SR-XPS and SERS as Probes for Structural Differences and Similarities. *Colloids Surf., A* **2017**, *532*, 183−188.
(47) Wiarachai, O.; Vilaivan, T.; Iwasaki, Y.; Hoven, V. P. Clickable and Antifouling Platform of Poly[(propargylmethacrylate)-*ran*-(2-methacryloyloxyethylphosphorylcholine)] for Biosensing Applications. *Langmuir* **2016**, *32*, 1184−1194.
(48) Chu, C.-W.; Higaki, Y.; Cheng, C.; Cheng, M.; Chang, C.; Chen, J.; Takahara, A. Zwitterionic Polymer Brush Grafting on Anodic Aluminum Oxide Membranes by Surface-Initiated Atom Transfer Radical Polymerization. *Polym. Chem.* **2017**, *8*, 2309−2316.
(49) Gupta, R. K.; Dunderdale, G. J.; England, M. W.; Hozumi, A. Oil/Water Separation Techniques: a Review of Recent Progresses and Future Directions. *J. Mater. Chem. A* **2017**, *5*, 16025−16058.

https://dx.doi.org/10.1021/acsomega.0c00259
ACS Omega 2020, 5, 7488−7496